Plant spectral diversity integrates functional and phylogenetic components of biodiversity and predicts ecosystem function

Article · May 2018

DOI: 10.1038/s41559-018-0551-1

CITATION
1

READS
429

8 authors, including:

Anna Katharina Schweiger
University of Minnesota
23 PUBLICATIONS **95** CITATIONS
SEE PROFILE

Jeannine Cavender-Bares
University of Minnesota Twin Cities
175 PUBLICATIONS **11,326** CITATIONS
SEE PROFILE

Philip A. Townsend
University of Wisconsin–Madison
165 PUBLICATIONS **3,694** CITATIONS
SEE PROFILE

Sarah E. Hobbie
University of Minnesota Twin Cities
253 PUBLICATIONS **19,218** CITATIONS
SEE PROFILE

ARTICLES
https://doi.org/10.1038/s41559-018-0551-1
nature ecology & evolution

Plant spectral diversity integrates functional and phylogenetic components of biodiversity and predicts ecosystem function

Anna K. Schweiger[1*], Jeannine Cavender-Bares[1*], Philip A. Townsend[2], Sarah E. Hobbie[1], Michael D. Madritch[3], Ran Wang[4], David Tilman[1,5] and John A. Gamon[4,6,7]

Biodiversity promotes ecosystem function as a consequence of functional differences among organisms that enable resource partitioning and facilitation. As the need for biodiversity assessments increases in the face of accelerated global change, novel approaches that are rapid, repeatable and scalable are critical, especially in ecosystems for which information about species identity and the number of species is difficult to acquire. Here, we present 'spectral diversity'—a spectroscopic index of the variability of electromagnetic radiation reflected from plants measured in the visible, near-infrared and short-wave infrared regions (400–2,400 nm). Using data collected from the Cedar Creek biodiversity experiment (Minnesota, USA), we provide evidence that the dissimilarity of species' leaf spectra increases with functional dissimilarity and evolutionary divergence time. Spectral diversity at the leaf level explains 51% of total variation in productivity—a proportion comparable to taxonomic (47%), functional (51%) or phylogenetic diversity (48%)—and performs similarly when calculated from high-resolution canopy image spectra. Spectral diversity is an emerging dimension of plant biodiversity that integrates trait variation within and across species even in the absence of taxonomic, functional, phylogenetic or abundance information, and has the potential to transform biodiversity assessment because of its scalability to remote sensing.

Assessing biodiversity in a concise and scalable manner is increasingly urgent in this era of accelerated global change, when over one-fifth of all vascular plant species are threatened[1], and the associated losses of ecosystem functions and services are expected to cost humanity 7% of the world's gross domestic product by 2050[2]. Diverse plant assemblages capture resources more efficiently, cycle nutrients more quickly and are more stable over time than depauperate ones[3,4]. The mechanisms that underpin the ecosystem benefits of biodiversity are a consequence of the functional differences among organisms[5,6], which promote complementary resource use[7–9], facilitation[8,10], population asynchrony[5,6] and resistance to disease[11]. While key individual traits provide competitive advantages and can enhance ecosystem function, particularly at low diversity levels, differences in multiple traits are often responsible for and perpetuate niche differences, which enables coexistence and can enhance ecosystem function, particularly at high diversity levels[9,12–14]. Quantifying the degree of functional variation in plant communities is thus critical for biodiversity research, and a number of functional diversity metrics have been developed[15,16]. There has been marked progress in recent decades in the understanding of the functional attributes of plants and their contribution to ecosystem function[12,13,17,18]. Nevertheless, choosing the most relevant traits to incorporate into a functional diversity metric that captures the functioning of a plant community in a particular area and at a certain time is challenging. Deciphering which traits to choose and the proper weighting of those traits is complicated by incomplete knowledge of interactions among individuals, the spatial and temporal distribution and variability of key limiting resources, and the seasonal and developmental shifts in a plant's resource requirements.

Phylogenetic diversity—a measure of the phylogenetic dissimilarity among species within an assemblage—has been proposed as a means to capture functional variation that avoids overemphasis of specific traits[19,20]. However, while functional differences are generally expected to increase with evolutionary divergence time[21], phylogenetic distance does not necessarily correspond to trait dissimilarity for any particular trait or the most relevant traits in a community[22,23]. On the one hand, traits can be phylogenetically conserved; for example, when close relatives have experienced strong environmental filtering[24], such that they share fundamental physiological strategies or ecological niches. On the other hand, traits can be labile; for example, when distant relatives show convergent evolution[25] or when close relatives show trait differentiation[23]. Depending on the traits considered and their level of evolutionary conservatism, the relationship between phylogenetic diversity and ecosystem function can thus be expected to vary along a continuum[23].

Ultimately, the positive effects of biodiversity on ecosystem function are a result of individual variation. Individuals interact with their abiotic and biotic environment, and intraspecific trait variability can reduce competition among individuals, allowing them to harness resources more completely[26,27]. In some cases, species' mean characteristics may capture the majority of functional variation in plant communities; for example, when differences among species exceed differences among individuals in a particular study area, or

[1]Department of Ecology, Evolution and Behavior, University of Minnesota, Saint Paul, MN, USA. [2]Department of Forest and Wildlife Ecology, University of Wisconsin–Madison, Madison, WI, USA. [3]Department of Biology, Appalachian State University, Boone, NC, USA. [4]Department of Earth and Atmospheric Sciences, University of Alberta, Edmonton, Alberta, Canada. [5]Bren School of Environmental Science and Management, University of California, Santa Barbara, CA, USA. [6]Department of Biological Sciences, University of Alberta, Edmonton, Alberta, Canada. [7]Center for Advanced Land Management Information Technologies, School of Natural Resources, University of Nebraska–Lincoln, Lincoln, NE, USA. *e-mail: aschweig@umn.edu; cavender@umn.edu

when the spatial scale of a study is large[27,28]. However, intraspecific variation within and among plant communities is often substantial and can even exceed interspecific variation[28]. Yet, incorporating intraspecific variation into functional or phylogenetic diversity metrics is often impractical[27].

Here, we present spectral diversity—a biodiversity metric based on spectra of electromagnetic radiation reflected from plants—that integrates a range of functional differences among individuals and species. Specifically, we investigated the extent to which (1) the dissimilarity of leaf-level spectra captures functional and phylogenetic differences among plant species and (2) the spectral diversity of plant communities, calculated from leaf-level and remotely sensed image spectra, predicts a critical ecosystem function: aboveground productivity.

Spectral reflectance profiles are continuous representations of the interaction between electromagnetic radiation and matter across a range of wavelengths. In the visible part of the spectrum (400–700 nm), light is predominantly absorbed by leaf pigments[29–31]. In the near-infrared (700–1,000 nm) and short-wave infrared (1,000–2,500 nm) regions, the absorption properties of cellular molecules (including water), as well as the internal and external structural characteristics of leaves, such as intercellular spaces, cell-wall thickness, waxiness of the cuticle and trichomes[29,31,32], influence how electromagnetic radiation is scattered and absorbed. At the whole-plant level, architectural and morphological characteristics, such as branching structure, leaf size, leaf clumping and leaf angle distribution also influence spectral reflectance[32]. The spectral differences among plants thus capture functional differences in chemical, anatomical and morphological traits. It follows that spectral diversity, similar to phylogenetic diversity when it is used as a proxy for functional diversity, provides an integrated measure of the variability of phenotypes within plant communities.

Our approach of using spectral diversity to predict ecosystem function builds on the spectral or optical diversity hypothesis[33–35], which suggests that species within a plant community occupy unique spectral spaces delineated by their chemical, anatomical and morphological characteristics. However, rather than using the number of spectrally distinct units to estimate the number of species or other taxonomic groups, our metric of spectral diversity describes the extent and filling pattern of the spectral space occupied by a plant community and thus its functional complexity. Analogous to functional trait space, spectral space is conceptually an *n*-dimensional hypervolume populated by spectra of species or individual plants measured at the leaf level or remotely. We describe the spectral diversity of a plant community based on the distances among species or individuals in spectral space. To compare plant communities, spectral diversity can be calculated based on a dissimilarity matrix of species' mean spectra and a community matrix of species presence/absence or abundance. Alternatively, spectral diversity can be calculated from separate dissimilarity matrices among spectra of individuals or remotely sensed image pixels for each community, which accounts for intraspecific variation (see Methods).

We collected spectral profiles of 17 species in 35 plots of the Cedar Creek biodiversity experiment[7,36] by measuring leaf-level reflectance with a spectrometer and leaf clip (see Methods and Supplementary Fig. 1). In the same plots, we acquired remotely sensed images using an imaging spectrometer mounted on an automated tram[37,38] (see Methods)—a form of proximal remote sensing that provides information similar to what could be obtained from unmanned aerial vehicles. We assessed species functional differences based on 14 foliar traits linked to resource capture rates (nitrogen, carbon, non-structural carbohydrates, hemicellulose, cellulose and lignin concentrations, and the content of chlorophyll a and b, β-carotene, lutein, neoxanthin, violaxanthin, antheraxanthin and zeaxanthin pigments; see Methods, Supplementary Fig. 2 and Supplementary Table 1) and determined species phylogenetic distances using the molecular phylogeny published in ref. [39] (see Methods). To calculate spectral, functional and phylogenetic diversity, we used functional trait dispersion ^{q}D(TM) (ref. [40]), which offers the flexibility to work with any dissimilarity matrix and can optionally include a community matrix of species abundance weights (see Methods). ^{q}D(TM) combines three components critical to biodiversity: the number of units per community (species, other phylogenetic or functional groups, individuals or image pixels, *S*), the regularity (evenness, ^{q}E(T)) and dispersion (distance from the community centroid, *M'*) of their distribution in mathematical space[40]. We calculated ^{q}D(TM) using species mean distances and a community matrix of proportional biomass per species, and set the Hill number to $q=1$ to make spectral, functional and phylogenetic diversity comparable with effective Shannon diversity—the exponential of the Shannon index. Additionally, we compared our results with non-abundance-weighted ^{q}D(TM), using a community matrix of species presence/absence instead of proportional biomass (see Methods), and with functional dispersion (FDis)[16]—a biodiversity metric that is independent of species richness by design. For the imaging spectrometer analysis, we calculated spectral diversity based on the dissimilarity of 1,000 randomly extracted vegetation pixels per plot without taking species identity, species richness or abundance into account.

Results

Spectral dissimilarity among species pairs increased with functional dissimilarity (Mantel test (999 replicates), coefficient of correlation (r) = 0.42, P = 0.001). On average, spectral dissimilarity among species pairs explained 28% of their distance in functional trait space (coefficient of determination (r^2) = 0.28, regression coefficient (b) = 0.62, t_{271} = 29.76, P < 0.001; Fig. 1a). We found increasing functional dissimilarity with spectral dissimilarity among species pairs for all but two focal species (Supplementary Fig. 3a and Supplementary Table 2). Spectral dissimilarity among species pairs also increased with evolutionary divergence time (Mantel test (999 replicates), r = 0.40, P = 0.001), probably because functional differences are a consequence of evolved differences. Previous studies have found many spectral regions to be phylogenetically conserved[41,42], and this is also the case for the species in our study (see Supplementary Methods and Supplementary Fig. 4). On average, spectral dissimilarity among species pairs explained 20% of their phylogenetic distance (r^2 = 0.20, b = 0.62, t_{271} = 27.72, P < 0.001; Fig. 1b). The relationship between spectral dissimilarity and phylogenetic distance for individual focal species revealed support for increasing spectral dissimilarity with phylogenetic distance for 13 out of 17 species (Supplementary Fig. 3b and Supplementary Table 2). The wavelengths contributing most to spectral dissimilarity among species (centre wavelengths 429, 675, 1,451, 1,981 and 2,360 nm; see Methods) aligned closely with known absorption features for chlorophylls (at 430 and 660 nm), carotenoids (at 430 nm), leaf water content (at 1,450 and 1,980 nm), proteins (at 1,980 and 2,350 nm) and cellulose (at 2,350 nm)[30,31,43] (Fig. 2), which are all traits associated with resource acquisition and partitioning in plant communities.

Spectral diversity of plant communities calculated from leaf-level spectra explained 51% of the total variation in productivity (r^2 = 0.51, b = 94.92, t_{33} = 5.90, P < 0.001; Fig. 3a). More productive communities were characterized by a greater number (Pearson's product correlation coefficient (r) = 0.72, t_{33} = 6.04, P < 0.001) of more dispersed (r = 0.74, t_{33} = 6.30, P < 0.001) and less evenly distributed (r = –0.40, t_{33} = –2.53, P = 0.02) species' mean spectra in spectral space. The dispersion of species' mean spectra predicted slightly more (r^2 = 0.55, b = 559.36, t_{33} = 6.30, P < 0.001; Supplementary Fig. 5c) of the total variation in productivity than the number of species (r^2 = 0.53, b = 22.86, t_{33} = 6.04, P < 0.001; Supplementary Fig. 5a), while the evenness of their distribution predicted less (r^2 = 0.16, b = –263.19, t_{33} = –2.53, P = 0.02; Supplementary Fig. 5b).

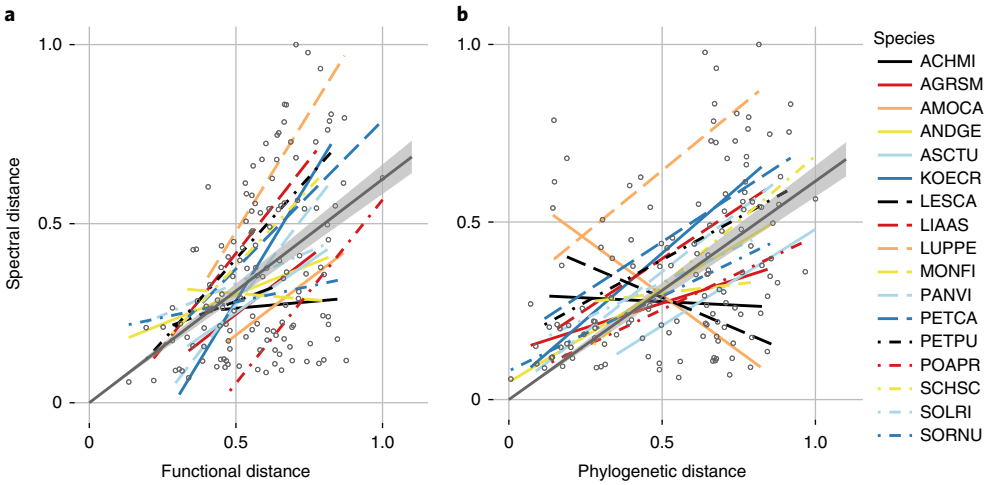

Fig. 1 | More functionally different and more distantly related species are more spectrally dissimilar. a,**b**, Spectral distance among all species pairs increased with functional distance ($n=273$, $r^2=0.28$, $b=0.62$, $t_{271}=29.76$, $P<0.001$; **a**) and phylogenetic distance ($n=273$, $r^2=0.20$, $b=0.62$, $t_{271}=27.72$, $P<0.001$; **b**). Relationships were predicted from linear regression models among all species pairs. The grey line is the fitted regression line for all species pairs; coloured lines represent fitted linear models for individual focal species paired with all other species; bands indicate 95% confidence intervals; and circles are species pairs. ACHMI, *Achillea millefolium* L.; AGRSM, *Agropyron smithii* Rydb.; AMOCA, *Amorpha canescens* Pursh; ANDGE, *Andropogon gerardii* Vitman; ASCTU, *Asclepias tuberosa* L.; KOECR, *Koeleria cristata* auct. non Pers. p.p.; LESCA, *Lespedeza capitata* Michx.; LIAAS, *Liatris aspera* Michx.; LUPPE, *Lupinus perennis* L.; MONFI, *Monarda fistulosa* L.; PANVI, *Panicum virgatum* L.; PETCA, *Petalostemum candidum* (Willd.) Michx.; PETPU, *Petalostemum purpureum* (Vent.) Rydb.; POAPR, *Poa pratensis* L.; SCHSC, *Schizachyrium scoparium* (Michx.) Nash; SOLRI, *Solidago rigida* L.; SORNU, *Sorghastrum nutans* (L.) Nash.

Spectral diversity, calculated based on the five most variable spectral bands located at the local maxima of the coefficient of variation, explained as much of the total variation in productivity as the full spectral profiles ($r^2=0.51$, $b=121.58$, $t_{33}=5.88$, $P<0.001$; Supplementary Fig. 6).

Spectral diversity of plant communities calculated from remotely sensed image spectra explained 41% of the total variation in productivity ($r^2=0.41$, $b=3.81$, $t_{25}=4.14$, $P<0.001$; Fig. 3b). Again, more productive communities were characterized by more dispersed spectra ($r=0.61$, $t_{25}=3.86$, $P<0.001$), while the correlation between productivity and the evenness of their distribution was not significant ($r=0.30$, $t_{25}=1.55$, $P=0.13$). The dispersion of image pixels in spectral space predicted more of the total variation in productivity ($r^2=0.37$, $b=3289.9$, $t_{25}=3.86$, $P<0.001$; Supplementary Fig. 7c) than the evenness of their distribution ($r^2=0.09$, $b=3{,}250.0$, $t_{25}=1.55$, $P=0.13$; Supplementary Fig. 7b); the number of spectra was constant at 1,000 randomly extracted image pixels per community (Supplementary Fig. 7a).

Overall, spectral diversity was as predictive of ecosystem function as functional, phylogenetic or taxonomic diversity. Functional diversity explained 51% of the total variation in productivity ($r^2=0.51$, $b=66.96$, $t_{33}=5.85$, $P<0.001$; Supplementary Fig. 8a)—the same proportion as spectral diversity—phylogenetic diversity explained 48% ($r^2=0.48$, $b=65.95$, $t_{33}=5.50$, $P<0.001$; Supplementary Fig. 8b) and effective Shannon diversity explained 47% ($r^2=0.47$, $b=35.80$, $t_{33}=5.38$, $P<0.001$; Supplementary Fig. 8c). Model performance ranked similarly (delta Akaike Information Criterion <3.2) and we found no combination of spectral, functional, phylogenetic or effective Shannon diversity that predicted productivity better than spectral diversity alone (Supplementary Table 3). These results were robust to the biodiversity metric used; both non-abundance-weighted ^{q}D(TM) (Supplementary Fig. 9) and FDis (Supplementary Fig. 10) explained comparable proportions of the total variation in productivity.

Discussion

Understanding and sustaining the contributions of plant biodiversity to ecosystem functions and services to humanity calls for integrative, consistent and scalable approaches to biodiversity research. Broad consensus has been reached that functional diversity is critical to ecosystem function[5–11] and functional traits have a tendency to be phylogenetically conserved[19–25]. Here, we provide evidence that the spectral dissimilarity of plants is coupled with their functional and evolutionary divergence, such that spectral diversity can be used to predict ecosystem function. Our results confirm previous findings that more productive plant communities are more functionally and phylogenetically diverse[5,6,19,20], but we also show that the spectral dissimilarity of plants captures this underlying functional variation resulting from contrasting evolutionary histories[44]. The links between spectral, functional and evolutionary divergence provide the rationale for using the dissimilarity of spectral profiles of plants to estimate biodiversity. Spectral diversity predicted the ecosystem consequences of biodiversity in our study system with as much or more explanatory power as functional, phylogenetic and taxonomic diversity. Moreover, spectral diversity can be calculated from remotely sensed image spectra without requiring information about species identity, richness or abundance.

The choice of which biodiversity measure is most appropriate for a particular study depends on data availability, as well as the goals, and spatial and temporal extent of the study. Taxonomic, phylogenetic and functional diversity can be readily calculated when species identities are known and phylogenetically resolved, or when accurate data on the plant traits critical to the ecosystem function of interest are available. However, spectral diversity of plant assemblages can provide unprecedented information about biodiversity and ecosystem function when the taxonomic identities, abundances and functional characteristics of plants are difficult to determine. Spectral information can be acquired relatively rapidly and consistently compared with measuring suites of functional traits based on traditional protocols. For assessing biodiversity repeatedly and over large spatial scales, spectral diversity can thus be advantageous, particularly as it accounts for intraspecific variation when calculated from randomly sampled leaf-level or remotely sensed spectra.

Intraspecific variability is increasingly recognized as an important contribution to ecosystem function[9,26–28]. However, there are reasons

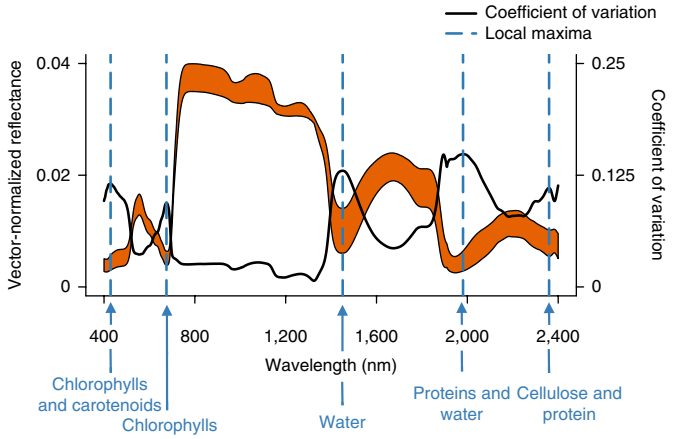

Fig. 2 | Spectral profiles, their coefficient of variation and local maxima of the coefficient of variation. The range of vector-normalized spectra of all species ($n=17$) is shown in red. The black line is the coefficient of variation of vector-normalized reflectance values for each spectral band ($n=2{,}000$). The blue vertical lines indicate five local maxima of the coefficient of variation (at 429, 675, 1,451, 1,981 and 2,360 nm); they align closely with known absorption features for chlorophylls (at 430 and 660 nm), carotenoids (at 430 nm), leaf water content (at 1,450 and 1,980 nm), proteins (at 1,980 and 2,350 nm) and cellulose (at 2,350 nm).

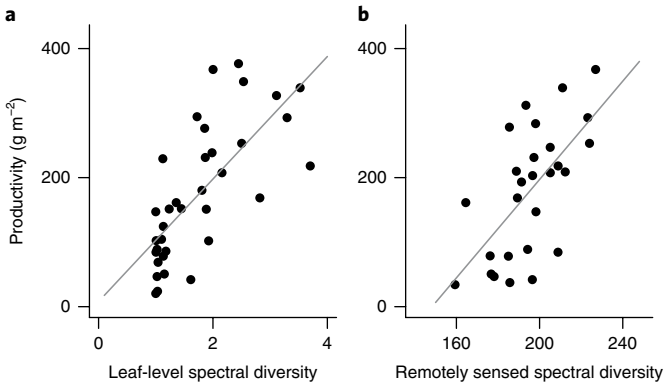

Fig. 3 | Relationship between spectral diversity and productivity. a,**b**, Aboveground productivity increased with spectral diversity of plant communities calculated from species' mean leaf-level spectra ($n=35$, $r^2=0.51$, $b=94.92$, $t_{33}=5.90$, $P<0.001$; **a**) and 1,000 randomly selected image pixels per plot acquired with an imaging spectrometer mounted on an automated tram ($n=27$, $r^2=0.41$, $b=3.81$, $t_{25}=4.14$, $P<0.001$; **b**). All relationships were predicted from linear regression models. The line is the fitted regression line, and each point represents a single plot in the Cedar Creek biodiversity experiment.

for using species' mean values over individual measurements in biodiversity metrics, including data availability, generalizability or under conditions where interspecific variation exceeds intraspecific variation. We used species' means for the leaf-level analysis to allow comparisons between functional, phylogenetic, taxonomic and spectral diversity. Furthermore, we sampled leaf-level reflectance of the most abundant species and thus did not have sufficient observations to incorporate individual variation, which we did when analysing the remotely sensed image spectra. At the leaf level, results for abundance-weighted and non-abundance-weighted versions of ^{q}D(TM) were consistent (Fig. 3 and Supplementary Figs. 8 and 9). It is known from previous analyses, and confirmed by our study, that aboveground productivity in the Cedar Creek biodiversity experiment can be well predicted by functional and phylogenic diversity, as well as by species richness[7,36,45] (Supplementary Fig. 8), because the experimental species pool consists of functionally dissimilar and distantly related species from different functional groups[7]. However, by decomposing ^{q}D(TM) into its three components, we show that the dispersion of the species distribution in spectral space (M') alone explains more of the total variation in productivity than the number of species (S), while the regularity of their distribution (^{q}E(T)) explains less (Supplementary Fig. 5). This result is confirmed by our remote-sensing analysis where the number of units (S) in spectral space (pixels per community) is constant (Supplementary Fig. 7). In addition, the relationships between biodiversity and productivity are similar when using FDis[16], which is independent of the number of species (Supplementary Fig. 10). Combined, these analyses reaffirm that functional differences among organisms promote ecosystem function and that these differences are associated with the amount and filling pattern of spectral space occupied by plant communities.

Spectral profiles can be considered integrative representations of plant phenotypes. It is well documented and supported by our study that spectra can accurately predict a range of chemical and morphological plant traits that are commonly used for determining functional diversity[31,43,46,47] (Supplementary Fig. 2 and Supplementary Table 1), but they also capture variation that is not traditionally measured. Regardless of whether plant traits are measured in situ or derived from databases, functional diversity metrics are frequently based on a small number of selected traits that are unlikely to fully capture the variation contributing to a particular ecosystem function. Spectral profiles still do not capture all critical aspects of a plant's phenotype and cannot directly account for important functional traits of organs that do not interact with light, such as seed mass or rooting depth. Nor are plant traits that are measured at the leaf level indicative of functional differentiation at the canopy level, such as plant height, growth architecture, total leaf area or spatial plant community composition. However, leaf spectra express many plant traits that are important for resource capture and stress tolerance including the contents of pigments, nutrients, water and the structure of leaves[31,43,46–49]. Thus, leaf spectra have an advantage over commonly measured traits in that they incorporate more of the total variation in function associated with leaf chemistry, anatomy and morphology, including variation that is difficult to measure or may be of unrecognized importance. Identifying the regions of the spectrum contributing most to spectral diversity provides a means to identify trait variation critical to ecosystem function (Fig. 2). While the spectral features of many chemical components have been described[30,31,43], the effects of anatomical and morphological characteristics on spectral reflectance are less well understood. Storing spectra in databases can enhance herbarium digitization efforts, enabling the investigation of changes in plant characteristics over time and allowing specimens to be revisited for future discovery of functional attributes critical for the structuring of plant communities.

Our analysis of canopy-level images acquired by the mobile tram in a manner analogous to measurements made by a low-flying unmanned aerial vehicle provides initial confirmation that remotely sensed spectral diversity of plant communities can predict ecosystem function. The spectra extracted from the tram's image pixels can be considered remotely sensed canopy measurements at leaf-level grain sizes that capture additional optical properties associated with varying leaf orientation and illumination in contrast with sampling spectra with a leaf clip. We expect the strength of the relationship between spectral diversity of plant communities and ecosystem function to decline with increasing pixel size as species spectra become progressively blended together. We also expect the spatial scale of this mixing effect to vary depending on the size of the plants in the community[38]. The imaging spectrometer mounted on the tram measured spectral reflectance from the visible region to the start of the near-infrared region of the electromagnetic spectrum

(430–925 nm). We do not yet know the degree to which additional information about macromolecules and canopy structure captured by wavelengths extending beyond 925 nm would influence this result[38,50]. The spectral and spatial scale dependence of the associations between spectral diversity and ecosystem function must be better understood if we are to design appropriate remote-sensing methods for biodiversity detection based on the diversity of plant traits. Further experimental work on exactly how leaf-level information is translated into image pixels at progressively coarser scales for different vegetation types will be important towards this end. As these issues are clarified, we anticipate that time series of spectral data that capture long-term changes in diversity and plant community function, and seasonal changes in plant physiology and phenology, will have the potential to transform our understanding of the ecosystem consequences of biodiversity on Earth.

Methods

Experiment. The Cedar Creek biodiversity experiment was planted at the Cedar Creek Ecosystem Science Reserve in East Bethel, Minnesota, in the summers of 1994 and 1995[7]. Plots measuring 9 m × 9 m were seeded with 1, 2, 4, 8 or 16 grassland–savannah perennial species selected from a pool of 18 species: 4 C_4 and 4 C_3 grasses, 4 legumes, 4 forb species and 2 tree species[7,36].

Spectral data. We collected leaf-level spectral reflectance measurements in 35 plots of the Cedar Creek biodiversity experiment, including all planted diversity levels from monocultures to 16 species plots, in the summer of 2015. We used a portable field spectrometer (SVC HR-1024i; Spectra Vista), covering the wavelength range 340 to 2,500 nm in 1,024 spectral bands, and a leaf clip with an internal light source (LC-RP PRO; Spectra Vista). We visually divided each plot into 9 3 m × 3 m subplots and collected spectral data within a randomly placed 1 m × 1 m grid in 4 to 8 subplots, depending on the planted diversity level; the centre subplot was always excluded to prevent disturbance (Supplementary Fig. 1). We placed the grid at least 50 cm away from the plot edges and measured 4 randomly selected individuals of the most abundant species per subplot. When the number of species per subplot was fewer than four, we sampled species repeatedly. When the number of species per plot was greater than four, we measured all species with more than 5% cover per plot by alternating the species sampled among subplots. We measured the reflectance of either three or five fully mature, healthy leaves per individual, depending on plant height. We measured three leaves for individuals under 30 cm in height—two from the top and one from the bottom canopy layer—and five leaves for individuals over 30 cm in height—two from the top, two from the mid- and one from the bottom canopy layer. Spectra were automatically calibrated for dark current and stray light, and referenced to the white calibration disc of the leaf clip approximately every 10 min. Spectral data processing included correcting artefacts at the sensor overlap regions around 900 nm and 1,900 nm (between the Si and first InGaAs sensor and between the first and second InGaAs sensor, respectively) and resampling to 1 nm spectral resolution. Noisy regions at the beginning and end of the spectrum (centre wavelengths smaller than 400 nm or greater than 2,400 nm) were excluded from analysis.

Proximal remote-sensing data were collected with an imaging spectrometer (E Series; Headwall Photonics) mounted on an automated tram[37]. Spectral images were successfully acquired along the northern edges of 27 of the 35 plots in July 2014 and 2015 (for details, see ref. [38]). The dataset consists of 1,000 × 1,000 pixel images covering the visible region to the beginning of the near-infrared region of the electromagnetic spectrum (400–990 nm) in 920 (2014) and 924 (2015) spectral bands. Spectra were resampled to 1 nm spectral resolution, and noisy regions at the beginning and end of the spectrum (centre wavelengths smaller than 430 nm or greater than 925 nm) were excluded from analysis. All spectral processing was performed using spectrolab 0.0.2[51] in R[52].

Functional traits. Leaf carbon and nitrogen content, carbon fractions, and pigment composition (see Supplementary Fig. 2 and Supplementary Table 1) of the same individuals used for leaf-level spectral analyses were predicted using partial least squares regression (PLSR) models[53] developed from chemical assays of leaf-tissue samples and corresponding reflectance spectra. Leaf-tissue samples were collected in the summers of 2015 and 2016 at the Cedar Creek Ecosystem Science Reserve and included 62 grassland–savannah species. Carbon and nitrogen contents (%) of oven-dried (at 65 °C for 48 h) samples were analysed with combustion–reduction elemental analysis (TruSpec CN Analyzer; LECO). Carbon fractions, including non-structural carbohydrates, hemicellulose, cellulose and lignin (%), were determined from oven-dried samples using sequential digestion (Fiber Analyzer 200; ANKOM Technology).

The content of chlorophyll a, chlorophyll b, β-carotene, lutein, neoxanthin, violaxanthin, antheraxanthin and zeaxanthin pigments (μmol m^{-2}) was determined using high-performance liquid chromatography (HPLC). Fresh leaf-tissue samples were cut with a hole punch and stored in liquid nitrogen. For extraction, leaf samples were ground in 80% acetone and centrifuged for 2 min at 13,000 r.p.m. The supernatant was collected with a syringe and the pellet re-extracted in 100% acetone and centrifuged again for 2 min at 13,000 r.p.m. The pooled supernatant was then filtered through a 0.45 μm nylon filter (Millex-HV; Millipore). Our HPLC system (Agilent 1200 Series; Agilent Technologies) included a diode array detector, quaternary pump and 250 mm × 4.6 mm octadecyl-silica column with 5 μm particle size (Allsphere ODS-1 Column; Grace). Solvent programmes were adapted from ref. [54]. We injected 20 μl pigment extract per sample and set the flow rate to 2 ml min^{-1}. Solvent A consisted of a mix of acetonitrile:methanol:0.1 M Tris pH 8.0 buffer (8:1:1). Solvent B consisted of a mix of methanol:ethyl acetate (68:32). Solvent A was run for 12 min followed by a 4 min gradient from solvent A to solvent B. Solvent B was run for 2 min followed by a 1 min gradient from solvent B to solvent A to reach column equilibrium. Peaks were detected at 445 nm and peak-area units were measured using ChemStation Software (Agilent Technologies). We calculated pigment concentrations from HPLC peak areas using calibration equations developed from HPLC peak-area units of pure pigments in dilution series, involving 8 steps for β-carotene, 14 steps for chlorophyll a and 16 steps for all other pigments, covering the entire expected range of pigment concentrations in our samples. Chlorophyll a, chlorophyll b and β-carotene were extracted from spinach with thin-layer chromatography[55] and re-dissolved in 100% acetone. Purified lutein was obtained from Sigma–Aldrich. The concentration of the pigment standards in dilution series were determined based on their absorbance measured with a UV-Vis spectrophotometer (Cary 50 Bio; Agilent Technologies) at 445 nm and corresponding extinction coefficients[56–59]. Calibration equations for neoxanthin, violaxanthin, antheraxanthin and zeaxanthin were based on normalized coefficients and lutein area units[60]. Pigment concentrations (ng mg^{-1}) were transformed to moles per unit area and standardized to chlorophyll content (μmol m^{-2} / total chlorophyll μmol m^{-2}). Chemical analyses were conducted at the University of Minnesota.

For PLSR modelling, we used plsRglm 1.1.1[61] in R[52] with the chemical component matrix as the dependent and the leaf spectra matrix as the predictor. Spectra were resampled to 20 nm spectral resolution and vector-normalized to correct for brightness differences, and wavelength ranges were limited to 1,100–2,400 nm for carbon and nitrogen, 1,200–2,400 nm for fibre[46], and 400–760 nm for pigment models. We performed 500 tenfold cross-validations and used the averaged PLSR coefficients for predictions. The number of PLSR components was minimized using the cross-validated predictive-residual-sum-of-squares (PRESS) criterion. Model performance was assessed based on the coefficient of determination (r^2) for linear regressions between measured and predicted values and the root mean squared error of prediction (RMSEP). For model statistics and value ranges, see Supplementary Fig. 2 and Supplementary Table 1.

Spectral, functional and phylogenetic distance. We assessed the association between species spectral, functional and phylogenetic distance using spectral, functional and phylogenetic dissimilarity matrices. The spectral dissimilarity matrix was based on Manhattan distances among species' mean spectra acquired at the leaf level. Manhattan distances accommodate the high degree of autocorrelation in spectral data. The functional dissimilarity matrix was based on Euclidean distances among *z*-standardized (zero mean, unit variance) species' mean foliar traits (see above; Supplementary Fig. 2 and Supplementary Table 1). The phylogenetic dissimilarity matrix was based on cophenetic distances calculated from the molecular phylogeny published in ref. [39] using the R package ape 3.3[62]. We assessed the overall correlation between the dissimilarity matrices with Mantel tests as implemented in ade4 1.-7[63], and fit linear regression models between the distances among all species pairs and for each species separately; that is, between each focal species' distance to all other species (Fig. 1, Supplementary Fig. 3 and Supplementary Table 2).

Diversity metrics and productivity. We calculated spectral, functional and phylogenetic diversity based on $^{q}D(TM)$[40], which uses a dissimilarity matrix and a community matrix of species presence/absence or abundance weights as input data. Defined as a quantity of distance, $^{q}D(TM)$ calculates the effective number of spectrally, functionally or phylogenetically distinct units in a community (which can be species, other phylogenetic or functional groups, individuals or image pixels) based on the number of units, the regularity (evenness) and dispersion of their distribution in mathematical space (see below). This allows spectral, functional, phylogenetic and taxonomic diversity to be compared and consistently interpreted. Leaf-level spectral diversity and all other biodiversity indices were based on species means and initially abundance weighted by proportional biomass (Fig. 3a and Supplementary Fig. 8). We set the Hill number in $^{q}D(TM)$ to $q = 1$ and calculated Shannon diversity using the R package vegan 2.4-1[64]. To identify the bands contributing most to spectral diversity, we calculated the coefficient of variation per wavelength across vector-normalized spectra (Fig. 2). We selected the bands located at five local maxima of the coefficient of variation to construct the spectral dissimilarity matrix and calculate spectral diversity, as described above (Supplementary Fig. 6). For comparison, we used species presence/absence data instead of proportional biomass to calculate the non-abundance-weighted version of $^{q}D(TM)$ for spectral, functional and phylogenetic diversity (Supplementary Fig. 9). Additionally, we calculated spectral, functional and phylogenetic diversity based on

FDis[16], which is by design independent of the number of species (Supplementary Fig. 10), using the R package FD 1.0-12[65]. For the imaging spectrometer analysis, we randomly extracted 1,000 vegetation pixels per imaged plot and calculated spectral diversity from the spectral dissimilarity matrices of all pixels, without including any information about species identity or abundance (Fig. 3b and Supplementary Fig. 7). Functional trait dispersion ${}^{q}D(TM)$ (ref. [40]) was calculated as:

$$ {}^{q}D(TM) = 1 + (S-1) \times {}^{q}E(T) \times M' $$

Evenness component : ${}^{q}E(T)$ Dispersion component : M'

$$ f_{ij} = \frac{d_{ij}}{\sum_i^S \sum_j^S d_{ij}} \qquad M = \sum_i^S \sum_j^S d_{ij} \times \frac{1}{S^2} $$

$$ {}^{q}H(T) = \left(\sum_i^S \sum_j^S f_{ij}^q \right)^{\frac{1}{1-q}} \qquad M' = M \times \frac{S}{S-1} $$

$$ {}^{q}D(T) = \frac{1 + \sqrt{1 + 4 \times {}^{q}H(T)}}{2} $$

including abundance weights:

$$ {}^{q}E(T) = \frac{{}^{q}D(T)}{S} \qquad M = Q = \sum (diag\,[\mathbf{comm}] \,\%\cdot\%\, [d_{ij}] \,\%\cdot\%\, diag\,[\mathbf{comm}]) $$

where f_{ij} is the proportional distance between distinct units i and j; d_{ij} is the functional, phylogenetic or spectral distance matrix between units i and j ($d_{ij} = d_{ji}$, $d_{ii} = 0$, range = (0, 1)); S is the number of units (range = (1, S); units can be species, other phylogenetic or functional groups, individuals or image pixels); ${}^{q}H(T)$ is the Hill diversity (q = Hill number); ${}^{q}D(T)$ is the effective number of equally distant units (range = (1, S); ${}^{q}E(T)$ is the regularity (evenness) of the dispersion of units in space; M' is the standardized mean dispersion (standardized distance from the centroid; range = (0, 1); M is the mean dispersion among all pairs of units (range = (0, $(S-1)/S$); Q is Rao's quadratic entropy; *diag* is the diagonal matrix of abundances in a community; and **comm** is the vector of abundances in a community.

Aboveground biomass data (g m^{-2} dry weight) per species were collected between 27 July and 4 August 2015. Observed species richness ranged from 5 to 20 species per plot. Spectral data were available for the 17 most abundant species, which we included in our analyses (for species names, see Fig. 1 and Supplementary Table 2). For the imaging spectrometer analysis, we additionally used aboveground biomass data (g m^{-2} dry weight) collected between 26 July and 1 August 2014 to match the year of image collection. We used aboveground biomass per plot as a measure of aboveground net primary productivity (referred to as 'productivity' throughout) and calculated linear regression models between productivity and each biodiversity metric. We also calculated multiple linear regressions based on all combinations of biodiversity metrics (Supplementary Table 3). We used differences in Akaike's information criterion to compare model performances and tested whether any diversity metric provided a significant parameter addition to a model based on likelihood ratio tests. We assessed the separate contribution of the three components of ${}^{q}D(TM)$ (the number of spectrally distinct units (S), the regularity (evenness, ${}^{q}E(T)$) and dispersion (M') of their distribution in spectral space) to the spectral diversity–productivity relationship based on Pearson's product correlation coefficients (r), and calculated linear regression models between each component of spectral diversity and productivity (Supplementary Figs. 5 and 7).

Reporting Summary. Further information on experimental design is available in the Nature Research Reporting Summary linked to this article.

Code availability. The R code for calculating ${}^{q}D(TM)$ was written by S. Kothari and is available at https://github.com/ShanKothari/DecomposingFD.

Data availability. Spectral and biomass data that support the findings of this study are available from EcoSIS (https://ecosis.org) and the Cedar Creek Ecosystem Science Reserve (http://www.cedarcreek.umn.edu/research/data). The tram dataset is available at https://doi.org/10.5067/Community/Headwall/HWHYPCCMN1MM.001.

Received: 10 July 2017; Accepted: 3 April 2018;
Published online: 14 May 2018

References

1. Anderson, S. et al. *State of the World's Plants 2016* (Royal Botanic Gardens, Kew, 2016).
2. Ten Brink, P. et al. in *The Cost of Policy Inaction: The Case of Not Meeting the 2010 Biodiversity Target* (eds Braat, L. & Ten Brink, P.) Ch. 6 (Alterra, Wageningen, 2008).
3. Cardinale, B. J. et al. Biodiversity loss and its impact on humanity. *Nature* **486**, 59–67 (2012).
4. Isbell, F. et al. Biodiversity increases the resistance of ecosystem productivity to climate extremes. *Nature* **526**, 574–577 (2015).
5. Tilman, D., Lehman, C. L. & Bristow, C. E. Diversity–stability relationships: statistical inevitability or ecological consequence? *Am. Nat.* **151**, 277–282 (1998).
6. Hector, A. et al. General stabilizing effects of plant diversity on grassland productivity through population asynchrony and overyielding. *Ecology* **91**, 2213–2220 (2010).
7. Tilman, D. et al. The influence of functional diversity and composition on ecosystem processes. *Science* **277**, 1300–1302 (1997).
8. Díaz, S. & Cabido, M. Vive la difference: plant functional diversity matters to ecosystem processes. *Trends Ecol. Evol.* **16**, 646–655 (2001).
9. Williams, L. J., Paquette, A., Cavender-Bares, J., Messier, C. & Reich, P. B. Spatial complementarity in tree crowns explains overyielding in species mixtures. *Nat. Ecol. Evol.* **1**, 0063 (2017).
10. Wright, A., Schnitzer, S. A. & Reich, P. B. Living close to your neighbors: the importance of both competition and facilitation in plant communities. *Ecology* **95**, 2213–2223 (2014).
11. Fargione, J. et al. From selection to complementarity: shifts in the causes of biodiversity–productivity relationships in a long-term biodiversity experiment. *Proc. R. Soc. B* **274**, 871–876 (2007).
12. Cadotte, M. W. Functional traits explain ecosystem function through opposing mechanisms. *Ecol. Lett.* **20**, 989–996 (2017).
13. Kraft, N. J., Godoy, O. & Levine, J. M. Plant functional traits and the multidimensional nature of species coexistence. *Proc. Natl Acad. Sci. USA* **112**, 797–802 (2015).
14. Zuppinger-Dingley, D. et al. Selection for niche differentiation in plant communities increases biodiversity effects. *Nature* **515**, 108–111 (2014).
15. Petchey, O. L., Hector, A. & Gaston, K. J. How do different measures of functional diversity perform? *Ecology* **85**, 847–857 (2004).
16. Laliberté, E. & Legendre, P. A distance-based framework for measuring functional diversity from multiple traits. *Ecology* **91**, 299–305 (2010).
17. Wright, I. J. et al. The worldwide leaf economics spectrum. *Nature* **428**, 821–827 (2004).
18. Adler, P. B., Fajardo, A., Kleinhesselink, A. R. & Kraft, N. J. Trait-based tests of coexistence mechanisms. *Ecol. Lett.* **16**, 1294–1306 (2013).
19. Maherali, H. & Klironomos, J. N. Influence of phylogeny on fungal community assembly and ecosystem functioning. *Science* **316**, 1746–1748 (2007).
20. Cadotte, M. W., Cardinale, B. J. & Oakley, T. H. Evolutionary history and the effect of biodiversity on plant productivity. *Proc. Natl Acad. Sci. USA* **105**, 17012–17017 (2008).
21. Felsenstein, J. Phylogenies and the comparative method. *Am. Nat.* **125**, 1–15 (1985).
22. Losos, J. B. Phylogenetic niche conservatism, phylogenetic signal and the relationship between phylogenetic relatedness and ecological similarity among species. *Ecol. Lett.* **11**, 995–1003 (2008).
23. Gravel, D. et al. Phylogenetic constraints on ecosystem functioning. *Nat. Commun.* **3**, 1117 (2012).
24. Ackerly, D. D. Community assembly, niche conservatism, and adaptive evolution in changing environments. *Int. J. Plant Sci.* **164**, S165–S184 (2003).
25. Cavender-Bares, J., Ackerly, D., Baum, D. & Bazzaz, F. Phylogenetic overdispersion in Floridian oak communities. *Am. Nat.* **163**, 823–843 (2004).
26. Bolnick, D. I. et al. Why intraspecific trait variation matters in community ecology. *Trends Ecol. Evol.* **26**, 183–192 (2011).
27. Violle, C. et al. The return of the variance: intraspecific variability in community ecology. *Trends Ecol. Evol.* **27**, 244–252 (2012).
28. Siefert, A. et al. A global meta-analysis of the relative extent of intraspecific trait variation in plant communities. *Ecol. Lett.* **18**, 1406–1419 (2015).
29. Ustin, S. L. et al. Retrieval of foliar information about plant pigment systems from high resolution spectroscopy. *Remote Sens. Environ.* **113**, S67–S77 (2009).
30. Curran, P. J. Remote sensing of foliar chemistry. *Remote Sens. Environ.* **30**, 271–278 (1989).
31. Jacquemoud, S. & Baret, F. PROSPECT: a model of leaf optical properties spectra. *Remote Sens. Environ.* **34**, 75–91 (1990).
32. Ollinger, S. V. Sources of variability in canopy reflectance and the convergent properties of plants. *New Phytol.* **189**, 375–394 (2011).
33. Asner, G. P. & Martin, R. E. Airborne spectranomics: mapping canopy chemical and taxonomic diversity in tropical forests. *Front. Ecol. Environ.* **7**, 269–276 (2008).
34. Rocchini, D. et al. Remotely sensed spectral heterogeneity as a proxy of species diversity: recent advances and open challenges. *Ecol. Informatics* **5**, 318–329 (2010).
35. Ustin, S. L. & Gamon, J. A. Remote sensing of plant functional types. *New Phytol.* **186**, 795–816 (2010).
36. Reich, P. B. et al. Impacts of biodiversity loss escalate through time as redundancy fades. *Science* **336**, 589–592 (2012).
37. Gamon, J. A., Cheng, Y., Claudio, H., MacKinney, L. & Sims, D. A. A mobile tram system for systematic sampling of ecosystem optical properties. *Remote Sens. Environ.* **103**, 246–254 (2006).

38. Wang, R.., Gamon, J. A.., Cavender-Bares, J.., Townsend, P. A.., & Zygielbaum, A. I.. The spatial sensitivity of the spectral diversity-biodiversity relationship: an experimental test in a prairie grassland. *Ecol. Appl.* **28**, 541–556 (2018).
39. Davies, T. J., Urban, M. C., Rayfield, B., Cadotte, M. W. & Peres-Neto, P. R. Deconstructing the relationships between phylogenetic diversity and ecology: a case study on ecosystem functioning. *Ecology* **97**, 2212–2222 (2016).
40. Scheiner, S. M.., Kosman, E.., Presley, S. J.., & Willig, M. R.. Decomposing functional diversity. *Methods Ecol. Evol.* **8**, 809–820 (2017).
41. McManus, K. M. et al. Phylogenetic structure of foliar spectral traits in tropical forest canopies. *Remote Sens.* **8**, 196 (2016).
42. Cavender-Bares, J. et al. Associations of leaf spectra with genetic and phylogenetic variation in oaks: prospects for remote detection of biodiversity. *Remote Sens.* **8**, 221 (2016).
43. Sims, D. A. & Gamon, J. A. Relationships between leaf pigment content and spectral reflectance across a wide range of species, leaf structures and developmental stages. *Remote Sens. Environ.* **81**, 337–354 (2002).
44. Cavender-Bares, J. et al. Harnessing plant spectra to integrate the biodiversity sciences across biological and spatial scales. *Am. J. Bot.* **104**, 966–969 (2017).
45. Cadotte, M. W., Cavender-Bares, J., Tilman, D. & Oakley, T. H. Using phylogenetic, functional and trait diversity to understand patterns of plant community productivity. *PLoS ONE* **4**, e5695 (2009).
46. Serbin, S. P., Singh, A., McNeil, B. E., Kingdon, C. C. & Townsend, P. A. Spectroscopic determination of leaf morphological and biochemical traits for northern temperate and boreal tree species. *Ecol. Appl.* **24**, 1651–1669 (2014).
47. Kokaly, R. F. & Clark, R. N. Spectroscopic determination of leaf biochemistry using band-depth analysis of absorption features and stepwise multiple linear regression. *Remote Sens. Environ.* **67**, 267–287 (1999).
48. Madritch, M. D. et al. Imaging spectroscopy links aspen genotype with below-ground processes at landscape scales. *Phil. Trans. R. Soc. B* **369**, 20130194 (2014).
49. Kothari, S. et al. Community-wide consequences of variation in photoprotective physiology among prairie plants. *Photosynthetica* **56**, 455–467 (2018).
50. Townsend, P. A.., Serbin, S. P.., Kruger, E. L.., & Gamon, J. A.. Disentangling the contribution of biological and physical properties of leaves and canopies in imaging spectroscopy data. *Proc. Natl Acad. Sci. USA* **110**, E1074 (2013).
51. Meireles, J. E., Schweiger, A. K. & Cavender-Bares, J. *spectrolab: class and methods for hyperspectral data* R package version 0.0.2 (2017); https://CRAN.R-project.org/package=spectrolab
52. R Development Core Team *R: A Language and Environment for Statistical Computing* (R Foundation for Statistical Computing, Vienna, 2016).
53. Wold, S., Martens, H. & Wold, H. in *Matrix Pencils (Lecture Notes in Mathematics)* (eds Ruhe, A. & Kagstrom, B.) 286–293 (Springer, Heidelberg, 1983).
54. Gilmore, A. M. & Yamamoto, H. Y. Resolution of lutein and zeaxanthin using a non-endcapped, lightly carbon-loaded C_{18} high-performance liquid chromatographic column. *J. Chromatogr. A* **543**, 137–145 (1991).
55. Quach, H. T., Steeper, R. L. & Griffin, G. W. An improved method for the extraction and thin-layer chromatography of chlorophyll a and b from spinach. *J. Chem. Educ.* **81**, 385 (2004).
56. Watanabe, T. et al. Preparation of chlorophylls and pheophytins by isocratic liquid chromatography. *Anal. Chem.* **56**, 251–256 (1984).
57. Zieger, R., & Egle, K. Zur quantitativen Analyse der Chloroplasten Pigmente. I. Kritische Überprüfung derspektralphotometrischen Chlorophyllbestimmung. *Beitr. Biol. Pflanz* **41**, 11–37 (1965).
58. Hiyama, T., Nishimura, M. & Chance, B. Determination of carotenes by thin-layer chromatography. *Anal. Biochem.* **29**, 339–342 (1969).
59. Aasen, A. & Jensen, S. L. Carotenoids of flexibacteria. IV. The carotenoids of two further pigment types. *Acta Chem. Scand.* **20**, 2322–2324 (1966).
60. De las Rivas, J., Abadía, A. & Abadía, J. A new reversed phase-HPLC method resolving all major higher plant photosynthetic pigments. *Plant Physiol.* **91**, 190–192 (1989).
61. Bertrand, F., Meyer, N. & Maumy-Bertrand, M. *Partial least squares regression for generalized linear models* R package version 1.1.1 (2014); https://CRAN.R-project.org/package=plsRglm
62. Paradis, E., Claude, J. & Strimmer, K. APE: analyses of phylogenetics and evolution in R language. *Bioinformatics* **20**, 289–290 (2004).
63. Dray, S. & Dufour, A.-B. The ade4 package: implementing the duality diagram for ecologists. *J. Stat. Softw.* **22**, 1–20 (2007).
64. Oksanen, J. et al. *vegan: community ecology package* R package version 2.4-1 (2016); https://CRAN.R-project.org/package=vegan
65. Laliberté, E., Legendre, P., Shipley, B. & Laliberté, M. E. *FD: measuring functional diversity from multiple traits, and other tools for functional ecology* R package version 1.0-12 (2010); https://CRAN.R-project.org/package=FD

Acknowledgements

We acknowledge B. Fredericksen for help with leaf-level sampling, HPLC and proof reading, I. Carriere for leaf-level sampling, C. Nguyen for chemical assays and HPLC, S. Kothari for carbon fraction analysis, H. Gholizadeh and B. Leavitt for curating the tram data, and M. Kaproth and E. Murdock for proof reading. Funding was provided by the National Science Foundation and National Aeronautics and Space Administration through the Dimensions of Biodiversity programme (DEB-1342872 grant to J.C.-B. and S.E.H., DEB-1342778 grant to P.A.T., DEB-1342827 grant to M.D.M., DEB-1342823 grant to J.A.G.), the Cedar Creek National Science Foundation Long-Term Ecological Research programme (DEB-1234162), iCORE/AITF (G224150012 and 200700172), NSERC (RGPIN-2015-05129), and CFI (26793) grants to J.A.G., and a China Scholarship Council fellowship to R.W.

Author contributions

This work is part of the Dimensions of Biodiversity project 'Linking remotely sensed optical diversity to genetic, phylogenetic and functional diversity to predict ecosystem processes', conceptualized by J.C.-B., P.A.T., S.E.H., M.D.M. and J.A.G. D.T. designed the Cedar Creek biodiversity experiment and advised on the project design. A.K.S. planned and conducted the data collection with input from J.C.-B., P.A.T. and J.A.G. J.A.G. designed the spectral tram and collected the tram data jointly with R.W. A.K.S. led the chemical analysis. A.K.S. analysed and interpreted the data with input from J.C.-B. A.K.S. wrote the manuscript. J.C.-B. edited the manuscript. P.A.T., S.E.H., M.D.M., D.T. and J.A.G. provided input to the manuscript at various stages.

Competing interests

The authors declare no competing interests.

Additional information

Supplementary information is available for this paper at https://doi.org/10.1038/s41559-018-0551-1.

Reprints and permissions information is available at www.nature.com/reprints.

Correspondence and requests for materials should be addressed to A.K.S. or J.C.-B.

Publisher's note: Springer Nature remains neutral with regard to jurisdictional claims in published maps and institutional affiliations.

nature research

Corresponding author(s): Anna K. Schweiger

Reporting Summary

Nature Research wishes to improve the reproducibility of the work that we publish. This form provides structure for consistency and transparency in reporting. For further information on Nature Research policies, see Authors & Referees and the Editorial Policy Checklist.

Statistical parameters

When statistical analyses are reported, confirm that the following items are present in the relevant location (e.g. figure legend, table legend, main text, or Methods section).

n/a	Confirmed	
☐	☒	The exact sample size (*n*) for each experimental group/condition, given as a discrete number and unit of measurement
☐	☒	An indication of whether measurements were taken from distinct samples or whether the same sample was measured repeatedly
☐	☒	The statistical test(s) used AND whether they are one- or two-sided *Only common tests should be described solely by name; describe more complex techniques in the Methods section.*
☐	☒	A description of all covariates tested
☐	☒	A description of any assumptions or corrections, such as tests of normality and adjustment for multiple comparisons
☐	☒	A full description of the statistics including central tendency (e.g. means) or other basic estimates (e.g. regression coefficient) AND variation (e.g. standard deviation) or associated estimates of uncertainty (e.g. confidence intervals)
☐	☒	For null hypothesis testing, the test statistic (e.g. *F*, *t*, *r*) with confidence intervals, effect sizes, degrees of freedom and *P* value noted *Give P values as exact values whenever suitable.*
☐	☒	For Bayesian analysis, information on the choice of priors and Markov chain Monte Carlo settings
☐	☒	For hierarchical and complex designs, identification of the appropriate level for tests and full reporting of outcomes
☐	☒	Estimates of effect sizes (e.g. Cohen's *d*, Pearson's *r*), indicating how they were calculated
☐	☒	Clearly defined error bars *State explicitly what error bars represent (e.g. SD, SE, CI)*

Our web collection on statistics for biologists may be useful.

Software and code

Policy information about availability of computer code

Data collection	Spectra Vista PC data acquisition software for collecting leaf-level spectra; Headwall Photonics Hyperspec III software for collecting imaging spectroscopy data with the mobile tram; Agilent ChemStation software for HPLC data collection.
Data analysis	R version 3.3.2; R packages ape 3.3, vegan 2.4-1, plsRglm 1.1.1, ade4 1.7-4, FD 1.0-12, picante 1.6-2, spectrolab 0.0.2; the R script for calculating qD(TM) is available at https://github.com/ShanKothari/DecomposingFD; ENVI 5.2 image processing software for extracting reflectance spectra from imaging spectroscopy data; Agilent ChemStation software for analysing HPLC data.

For manuscripts utilizing custom algorithms or software that are central to the research but not yet described in published literature, software must be made available to editors/reviewers upon request. We strongly encourage code deposition in a community repository (e.g. GitHub). See the Nature Research guidelines for submitting code & software for further information.

Data

Policy information about availability of data

All manuscripts must include a data availability statement. This statement should provide the following information, where applicable:

- Accession codes, unique identifiers, or web links for publicly available datasets
- A list of figures that have associated raw data
- A description of any restrictions on data availability

Spectral and biomass data that support the findings of this study (Figs. 1-3; Supplementary Figs. 3-10) are available from EcoSIS (https://ecosis.org) and the Cedar Creek Ecosystem Science Reserve (http://www.cedarcreek.umn.edu/research/data). The tram dataset is available from the LP DAAC (doi: 10.5067/Community/Headwall/HWHYPCCMN1MM.001).

Field-specific reporting

Please select the best fit for your research. If you are not sure, read the appropriate sections before making your selection.

☐ Life sciences ☐ Behavioural & social sciences ☒ Ecological, evolutionary & environmental sciences

For a reference copy of the document with all sections, see nature.com/authors/policies/ReportingSummary-flat.pdf

Ecological, evolutionary & environmental sciences study design

All studies must disclose on these points even when the disclosure is negative.

Study description	Reflectance spectra of plants were collected using a portable spectrometer with a leaf clip and an imaging spectrometer mounted on an automated tram system, respectively. We tested if more spectrally dissimilar species were more functionally dissimilar and more distantly related, and investigated the degree to which the spectral diversity of plant communities predicted aboveground productivity, a critical ecosystem function.
Research sample	Leaf-level spectra were collected in 35 plots and imaging spectrometry data were collected in 27 plots in the Cedar Creek Biodiversity experiment in East Bethel, Minnesota. This subset of plots is annually sampled for aboveground biomass and covers all initially planted diversity levels. The experiment was seeded in the summers of 1994 and 1995 with 1, 2, 4, 8 or 16 grassland–savannah perennial species selected from a pool of 18 species: 4 C4 and 4 C3 grasses, 4 legumes, 4 forb species and 2 tree species. Plots measure 9 m × 9 m. We included the 17 most abundant species in our study: Achillea millefolium L., Agropyron smithii Rydb., Amorpha canescens Pursh, Andropogon gerardii Vitman, Asclepias tuberosa L., Koeleria cristata auct. non Pers. p.p., Lespedeza capitata Michx., Liatris aspera Michx., Lupinus perennis L., Monarda fistulosa L., Panicum virgatum L., Petalostemum candidum (Willd.) Michx., Petalostemum purpureum (Vent.) Rydb., Poa pratensis L., Schizachyrium scoparium (Michx.) Nash, Solidago rigida L. and Sorghastrum nutans (L.) Nash.
Sampling strategy	To capture species variability within each plot, we visually divided each plot into nine 3 m x 3 m subplots and measured the most abundant species in 4 to 8 subplots per plot (4 subplots for 1 and 2 species plots, 6 subplots for 6 species plots, and 8 subplots for 8 or 16 species plots). To capture spectral variability within individuals, we took either three or five spectral measurements of different leaves per individual depending on plant height, three measurements for individuals < 30 cm and five measurements for individual >=30 cm (see Methods). The plots sampled with the mobile tram system were the same as for the leaf-level data collection, with the exception of six plots in which tram data collection failed due to technical difficulties and two plots were no data were collected because of time and weather constraints.
Data collection	Leaf-level spectra were collected by A.K.S, Brett Fredericksen and Ian Carriere using a spectrometer covering the wavelength region 340–2500 nm and a leaf clip. The tram data were collected by R.W. and J.A.G. using an imaging spectrometer covering the wavelength region 400–990 nm, mounted on an automated tram system designed by J.A.G. (see Methods).
Timing and spatial scale	Leaf-level data were collected between July, 2nd and July, 22nd 2015. Tram data were collected between July, 23rd and July, 30th 2014 and between July, 8th and July, 26th 2015, respectively. The timing of spectral data collection on the ground matched the timing of airborne imaging spectrometer campaigns that are part of the Dimensions of Biodiversity project “Linking remotely sensed optical diversity to genetic, phylogenetic and functional diversity to predict ecosystem processes”. We collected spectral data at the leaf level and the proximal canopy level (at around 3 m above ground). Aboveground productivity was measured and predicted at the plant community scale.
Data exclusions	No data were excluded from the analyses.
Reproducibility	Spectral, functional and phylogenetic diversity of plant communities was calculated using three different methods which all provided consistent results: 1) abundance-weighted functional trait dispersion qD(TM) (Scheiner, S. M., Kosman, E., Presley, S. J. & Willig, M. R., 2016), 2) non-abundance-weighted qD(TM) and 3) functional dispersion FDis (Laliberte & Legendre, 2010). Spectra collected with the mobile tram are not a true replicate of spectra collected with a leaf clip. However, the tram data were collected in the same research plots as the leaf-level spectra, and albeit the tram measures spectral reflectance at a different scale, the total amount of variability in aboveground productivity explained by spectral diversity calculated from the tram data was comparable.

Randomization	Species composition of the plots was determined by random draws of 1, 2, 4, 8, or 16 species from a pool of 18 species. For the leaf-level sampling, we visually divided each plot into nine 3 m x 3 m subplots and collected spectral data within a randomly placed 1 m x 1 m grid in 4 to 8 subplots (see Methods). We measured four randomly selected individuals of the most abundant species per subplot. For the imaging spectrometer data analysis, we extracted 1,000 vegetation pixels per imaged plot at random. To predict foliar chemistry from leaf-level spectra, we calibrated partial least squares regression (PLSR) models for a set of 14 leaf traits. Models were tenfold cross-validated 500 times and model coefficients were averaged for predictions (see Methods).
Blinding	NA; there were no treatments assigned and data were not grouped.

Did the study involve field work? ☒ Yes ☐ No

Field work, collection and transport

Field conditions	All data were collected under dry weather conditions. Tram data were collected under sunny skies.
Location	All data were collected at the Cedar Creek Ecosystem Science Reserve in East Bethel, Minnesota, USA (45.403000, -93.190000).
Access and import/export	All sampling efforts were coordinated with Cedar Creek staff.
Disturbance	We did not step into the plots and always set up our equipment outside of the plots. For leaf-level data acquisition, we visually divided each plot into nine subplots and collected spectra in four to eight subplots; the centre subplot was always excluded to prevent disturbance.

Reporting for specific materials, systems and methods

Materials & experimental systems

n/a	Involved in the study
☒	☐ Unique biological materials
☒	☐ Antibodies
☒	☐ Eukaryotic cell lines
☒	☐ Palaeontology
☒	☐ Animals and other organisms
☒	☐ Human research participants

Methods

n/a	Involved in the study
☒	☐ ChIP-seq
☒	☐ Flow cytometry
☒	☐ MRI-based neuroimaging